Biophysical Chemistry, 43 (1992) 29–37
Elsevier Science Publishers B.V., Amsterdam

BIOCHE 01648

Phase transitions of phospholipid vesicles under osmotic stress and in the presence of ethylene glycol

Masahito Yamazaki, Masato Ohshika, Naoto Kashiwagi and Tsutomu Asano
Department of Physics, Faculty of Science, Shizuoka University, Shizuoka 422 (Japan)

(Received 12 May 1991; accepted in revised form 17 October 1991)

Abstract

The effects of poly(ethylene glycol) (PEG) on the phase transition of phospholipid multilamellar vesicles (MLVs) were investigated by using differential scanning calorimetry (DSC). Main transition temperature (T_m) and the pre-transition temperature (T_p) of neutral phospholipid-, DMPC- [1], DPPC- and DSPC-MLVs increased with an increase in PEG concentration. The subtransition temperature of DPPC-MLV also increased with an increase in PEG concentration. These results could be qualitatively explained by enhancement of the lateral packing on the basis of the osmoelastic coupling theory. The pretransition temperature increased faster than the main transition temperature did with an increase in PEG concentration. The increment of T_m depended on the hydrocarbon chain length, the shorter the hydrocarbon chain length was, the larger the increment was. The transition width in the DSC peak was broadened with an increase in PEG concentration. These three above-mentioned effects are the main differences between the effects of the osmotic stress on the phase transition of MLVs and those of hydrostatic pressure. On the other hand, ethylene glycol (EG), which is the monomer of PEG, had a biphasic effect on transition temperature of DPPC-, DSPC-, and DMPC-MLV, reducing T_m and T_p at low concentrations, but increasing T_m and extinguishing pretransition at high concentrations. This is explained by the induction of an interdigitated gel phase at high concentrations of EG, which indicates that EG can easily penetrate into the head group region of the lipid, in contrast with PEG 6K, because EG is small. Temperature–EG concentration phase diagrams for the various PC-MLVs were determined. The minimum concentration of EG where interdigitation occurs is largely dependent on the hydrocarbon chain length.

Keywords: Thermotropic phase transition: Phospholipids; Poly(ethylene glycol); Osmoelastic coupling; Ethylene glycol; Interdigitated gel phase

1. Introduction

High molecular weight poly(ethylene glycol) (PEG) is a water-soluble fusogen which has been used frequently to fuse somatic cells [1–4]. It also causes aggregation of phospholipid vesicles and, at relatively high concentrations, induces fusion

Correspondence to: Dr. Masahito Yamazaki, Department of Physics, Faculty of Science, Shizuoka University, Shizuoka 422, Japan. Fax: 81-(0)54-237-9895.

[1] Abbreviations: DSC, differential scanning calorimetry; DMPC, 1,2-dimirystoyl-*sn*-glycero-3-phosphatidylcholine; DPPC, 1,2-dipalmitoyl-*sn*-glycero-3-phosphatidylcholine; DSPC, 1,2-distearoyl-*sn*-glycero-3-phosphatidylcholine; PIPES, piperazine-*N*,*N*′-bis (2-ethanesulfonic acid)

[5–9]. To understand the interaction of PEG with biological membranes, the thermotropic phase transition of vesicles of dipalmitoylphosphatidylcholine (DPPC) in the presence of PEG was studied [10]. According to that study, PEG causes concentration-dependent increase in main transition temperature (T_m). However, a reasonable interpretation of this effect of PEG was not given.

Recently, we have proposed a novel concept of osmoelastic coupling in biomembranes [8,11]. In a suspension of phospholipid vesicles containing a high molecular weight PEG, the PEG molecules are preferentially excluded from the region adjacent to the vesicle surface (exclusion layer), but small molecules such as water or inorganic ions are not excluded. Such exclusion induces an osmotic stress onto the vesicle membranes, which increases with an increase in PEG concentration. In an equilibrium state, the membranes of the vesicles are compressed to produce elastic pressure which counterbalances the osmotic stress (osmoelastic coupling). This concept can reasonably explain many phenomena observed in other biological systems [9,12–14]. For the case of multilamellar vesicles (MLV) of neutral phospholipds, all the lipid bilayer membranes in the MLV are equally compressed laterally [11].

In this report, we investigated effects of PEG on the phase transitions of MLV of neutral phospholipid, and explained these effects on the basis of the osmoelastic coupling theory. We also studied the effects of ethylene glycol (EG), which is a monomer of PEG, on the phase transition of MLV as a control experiment, and determined temperature–EG concentration phase diagrams.

2. Materials and methods

1,2-Dipalmitoyl-*sn*-glycero-3-phosphatidylcholine (DPPC) and 1,2-dimirystoyl-*sn*-glycero-3-phosphatidylcholine (DMPC) were purchased from Sigma Chemical Co. 1,2-Distearoyl-*sn*-glycero-3-phosphatidylcholine (DSPC) was purchased from Funakoshi Co. and PEG 6K (average molecular weight 7,500 Da) and ethylene glycol were purchased from Wako Chemical Co.

Multilamellar vesicles (MLVs) were prepared by adding the appropriate amounts of PIPES buffer (10 m*M* PIPES, pH 7.5, 140 m*M* NaCl) to the dry lipid and then heating the mixture to about 10°C above the main transition temperature for 20 min. During the incubation time, the suspension was vortexed for about 1 min several times. To investigate the effect of the osmotic stress, PEG 6K solution or ethylene glycol solution added the preformed MLV solution, and the mixture was incubated at about 10°C above the main transition temperature for 1 hour (PEG) or 2 hours (EG) to attain equilibrium.

For the experiments of subtransitions, MLV suspensions were stored at 4°C for 7 days and then mixed with PEG 6K solution or buffer and incubated for 24 hours at 4°C. They were transferred to calorimetry pans at 4°C and loaded at 2°C into the precooled scanning calorimeter.

Differential scanning calorimetry (DSC) experiments were performed using a Rigaku DSC-8230B instrument. Usually, each sample was heated at a rate of 2.0°C/min. Two kinds of phase transition temperatures were determined not only the usual one at the onset of the endothermic transition extrapolated to the baseline but also the one at the maximum of endothermic transition peak. Each sample was scanned several times over (for the experiment of subtransition, there was only one heating scan.). The transition temperature was determined by averaging these measurements. The sample contained 0.2 μmol of the lipids and the reference contained an appropriate amount of the buffer solution were packed in the DSC pans. The concentrations of lipid in the sample were determined by the phosphate analysis [15].

X-ray diffraction experiments were performed by using Nickel filtered CuK_α X-radiation (λ = 1.54 Å) from rotating anode type X-ray generator (Rigaku, Rotaflex, RU-300). X-ray diffraction data were recorded using a position sensitive proportional counter (Rigaku, PSPC-5) and associated electronics (position analyzer, multichannel analyzer, etc., Rigaku). In all cases, samples were sealed in a thin-walled glass capillary tube (outer diameter 1.0 mm) and mounted in a thermostatable holder whose stability was ±0.5°C.

3. Results

DSC heating curves of DMPC-MLV in the presence of PEG 6K are shown in Fig. 1. There were two endothermic transition peaks in the absence of PEG 6K, which correspond to pre-, and main transition. The main transition temperature T_m and pre-transition temperature T_p (onset temperatures) were 14.1°C and 23.8°C, respectively. As shown in Fig. 2, T_m and T_p increased with an increase in PEG 6K concentration. The increase of T_p was much larger than that of T_m at the same concentration of PEG 6K. The increments of T_m and T_p (onset temperature), for example, at 40% (w/v) of PEG 6K were 1.5°C and 7.7°C on heating at 2°C/min, respectively. They did not depend on the heating rate in the range of 1°C/min to 4°C/min. The pre-transition peak disappeared above 48% (w/v) PEG 6K. The enthalpy change of main transition (ΔH) was almost equal in the concentration range up to 40% (w/v) within experimental accuracy. Their average value was 6.6 kcal/mol, showing good agreement with the reported value of pure DMPC-MLV [16]. However, it abruptly changed to 8.3 kcal/mol above 48% (w/v). The increment of ΔH almost equals to the enthalpy change of pre-transition. The half width of main transition slightly increased with an increase in PEG concentration.

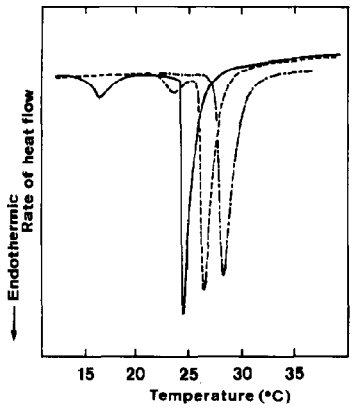

Fig. 1. Differential scanning calorimetry heating curves of DMPC-MLV in the presence of PEG 6K. (———) 0%, (- - - - -) 40%, and (— — —) 54% (w/v) PEG 6K. Heating rates were 2°C/min.

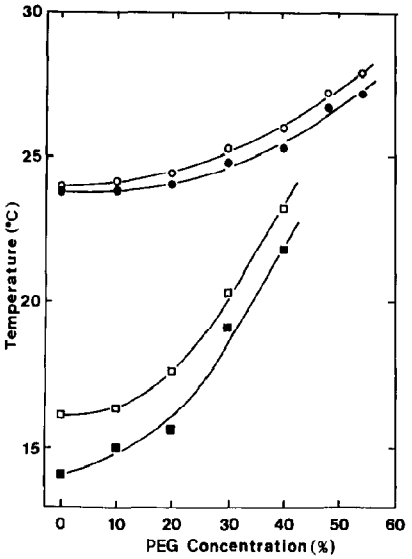

Fig. 2. Temperatures of main transition (●, ○) and pre-transition (■, □) of DMPC-MLV in the presence of PEG 6K. Heating rates were 2°C/min. Solid symbols represent transition onset temperatures and open symbols represent temperatures of endotherm maxima.

We obtained similar results from the experiments of DPPC-MLV and DSPC-MLV. In the absence of PEG, T_p and T_m were 35.6°C and 41.3°C for DPPC-MLV, and 49.9°C and 53.9°C for DSPC-MLV, respectively. These temperatures of DPPC- and DSPC-MLV also increased with an increase in PEG 6K concentration. The increment of main transition temperature (ΔT_m) depended strongly on the hydrocarbon chain length. The shorter the chain of the lipid, the larger the T_m the MLV will have (Fig. 3). For example, at 48% (w/v) PEG 6K, ΔT_m were 2.9°C, 2.0°C and 1.7°C for DMPC (C_{14}), DPPC (C_{16}) and DSPC (C_{18}), respectively. They did not depend on the heating rate in the range of 1°C/min to 4°C/min. The increments of T_p were much larger than that of T_m at the same concentration of PEG 6K for DPPC- and DSPC-MLV as well as DMPC-MLV. The characteristic properties of the enthalpy change and the half width of main tran-

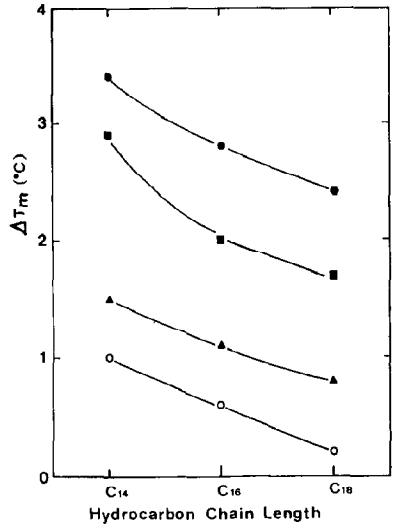

Fig. 3. The dependence of the increments of main transition (onset) temperature (ΔT_m) on hydrocarbon chain length in the presence of PEG 6K. (○) 30%, (▲) 40%, (■) 48%, and (●) 54% (w/v). C_{14} denotes DMPC, C_{16} DPPC, and C_{18} DSPC.

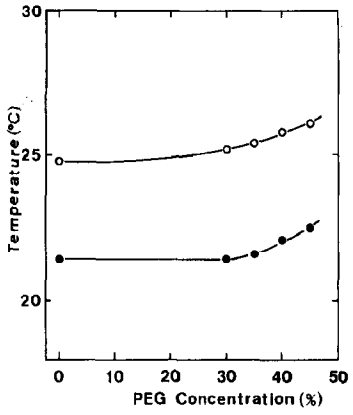

Fig. 4. Temperatures of subtransition of DPPC-MLV in the presence of PEG 6K. Onset temperatures (●); temperatures of endotherm maxima (○). See Section 2 for details on the preparation of samples.

sition of DPPC-MLV were the same as those of DMPC-MLV.

At a temperature lower than the pre-transition temperature, sub-transition of DPPC-MLV is known to occur after prolonged storage at 4°C [17]. The temperature of sub-transition of DPPC-MLV which was incubated at 4°C for one week was 21.4°C in the absence of PEG 6K on heating at 2°C/min. It also increased with an increase in PEG 6K concentration (Fig. 4). The increment of this onset temperature at 40% (w/v) was 0.5°C.

Effects of ethylene glycol (EG; the monomer of PEG) on the phase transition of DPPC-MLV were investigated to compare them with those of PEG. As shown in Fig. 5, T_m of DPPC-MLV decreased slightly with an increase in EG concentration below 30% (w/v). Then it increased slightly above 40% (w/v). The pre-transition temperature of DPPC-MLV largely decreased with an increase in EG below 30% (w/v). The repeating period (spacing) of DPPC-MLV at 20°C in the absence of EG was 64 Å, which agrees with the reported value [18]. It increased slightly with increasing EG concentration, and then rapidly decreased from 66 Å to 49 Å around 36% (w/v) (Fig. 6). Two kinds of first-order diffraction peaks were observed between 34% and 36% (w/v). Wide-angle reflections of DPPC-MLV at 20°C

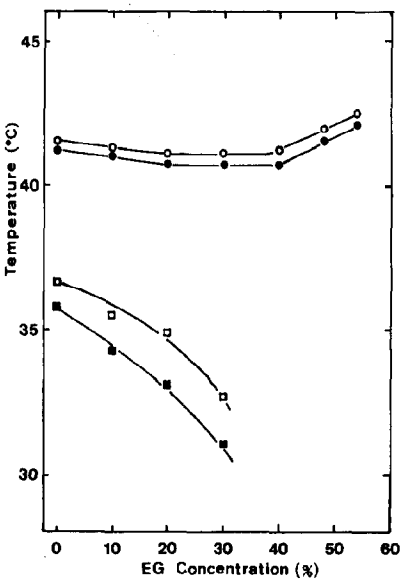

Fig. 5. Temperatures of main transition (●, ○) and pre-transition (■, □) of DPPC-MLV in the presence of ethylene glycol (EG). Heating rates were 2°C/min. Solid symbols represent transition onset temperatures and open symbols represent temperatures of endotherm maxima.

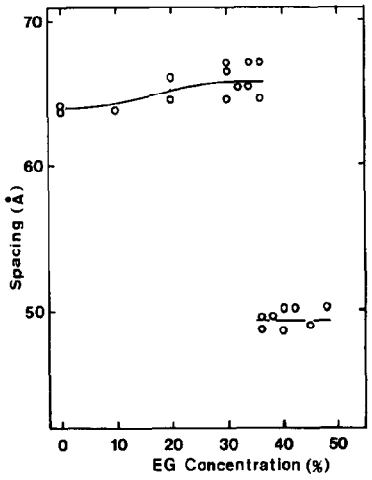

Fig. 6. Lamellar repeat periods (spacing) of DPPC-MLV at 20°C in the presence of EG.

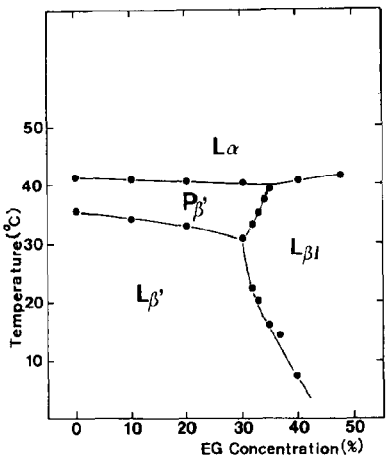

Fig. 7. Temperature–EG concentration phase diagram for DPPC-MLV; T_m and T_p were determined by the DSC method in Fig. 5. Other transition temperatures were determined by small-angle X-ray scattering.

with EG concentrations from 0% to 30% (w/v) consisted of a sharp reflection at 4.22 Å and a diffuse reflection centered at 4.14 Å, which are characteristic of the $L_{\beta'}$ phase [18]. Above 40% (w/v) EG, the wide-angle pattern showed a single sharp reflection at 4.10 Å. A sudden and large decrease (15 Å) of the repeating period and the characteristic of the wide-angle reflection pattern indicate that the MLV in high concentrations of EG was in the interdigitated gel phase ($L_{\beta I}$ phase) [19].

The temperature–EG concentration phase diagram for DPPC-MLV (Fig. 7) was determined

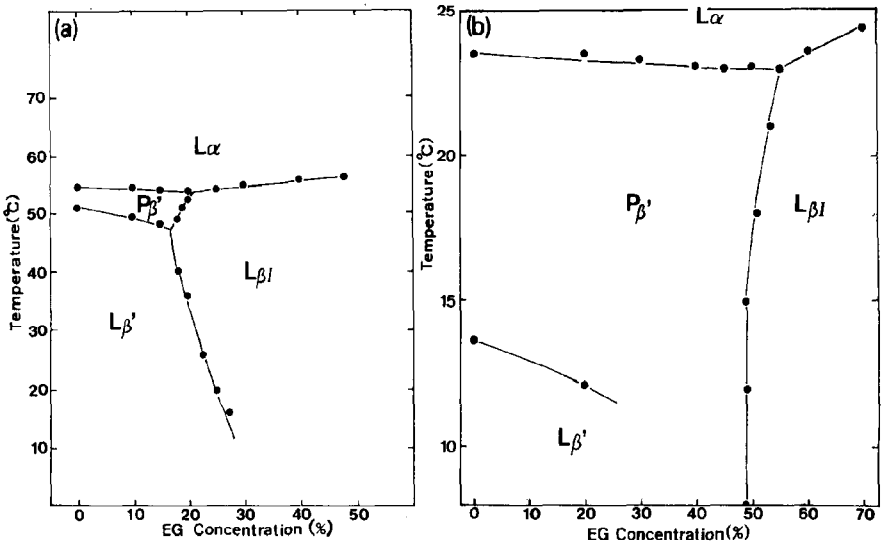

Fig. 8. Temperature–EG concentration phase diagram for DSPC-MLV (a) and DMPC-MLV (b); T_m and T_p were determined by the DSC method. Other transition temperatures were determined by small-angle X-ray scattering.

by means of an X-ray diffraction method and a DSC method (Fig. 5). In the X-ray diffraction method, phase boundaries were determined by monitoring changes in the strong first-order diffraction peak and temperature was increased in small steps (1 or 2°C) at the same concentration (C) of EG after the equilibrium was attained. This phase diagram can be divided into three regions. In the region of low concentration (Region A: $C < 30\%$), the phase changes from $L_{\beta'} \rightarrow P_{\beta'} \rightarrow L_{\alpha}$ as the temperature raises. In the region of medium concentration (Region B; $30\% < C < 38\%$), it changes from $L_{\beta'} \rightarrow L_{\beta I} \rightarrow P_{\beta'} \rightarrow L_{\alpha}$. In the region of high concentration (Region C; $C > 38\%$), it changes from $L_{\beta'} \rightarrow L_{\beta I} \rightarrow L_{\alpha}$. The rate of phase transition from $L_{\beta'}$ to $L_{\beta I}$ at the same concentration of EG was very low (order of minutes). Temperature–EG concentration phase diagrams of DSPC- and DMPC-MLV were also determined in the same way as that of DPPC-MLV (Fig. 8).

4. Discussion

The temperatures of the phase transitions of DMPC-, DPPC- and DSPC-MLV increased with an increase in PEG 6K concentration, which agrees with the results of the interaction of DPPC-MLV with PEG [10]. This mechanism might be explained by the direct interaction of PEG with the membranes. However, in the DSC thermograms, there was only one peak found for each phase transition (the main transition and the pre-transition) in the presence of PEG 6K. If PEG 6K binded to the lipid head group and thereby the phase transition temperature increased as indicated in the case of DPPC-Ca^{2+} system [20], the effect of PEG might be confined to the outer bilayer because it cannot enter into the MLV. Hence there should be two peaks for each phase transition in the DSC thermograms, one of which comes from the outermost bilayer and the other from the inner bilayers. Consequently, our results contradict the above supposition. These analyses also indicate indirectly that PEG did not bind to the lipid bilayer membranes if the binding of PEG had an effect on the phase transition of the MLV. Moreover, we have proposed the "osmoelastic coupling" theory; high molecular weight PEG molecules are preferentially excluded from the region adjacent to the vesicle surface, which induces the osmotic stress [8]. Recently, the preferential exclusion of PEG from the surface of phospholipid membranes was also indicated by the electrophoretic mobility experiments [21]. Therefore the mechanism of the increase in the phase transition temperature induced by PEG cannot be explained by the direct interaction of PEG with the membrane.

In the case of single-bilayer vesicles which are completely closed, the addition of membrane impermeable solutes caused the hydrostatic pressure difference according to Van't Hoff's law and a tangential stress in the plane of the membrane increases with an increase in the solute concentration [40,41], and consequently, this stress may raise the transition temperature. However, in the case of MLV, small molecules can enter the aqueous region between bilayers of MLV after a long incubation time owing to incomplete vesicular structures [11,26] and, as a result, there is no hydrostatic pressure difference. Therefore the hydrostatic pressure difference cannot explain this mechanism.

The increase of the phase transition temperatures can be qualitatively explained on the basis of the osmoelastic coupling theory [8,11]. Since PEG 6K cannot enter into inside of the MLV owing to the steric hindrance, the chemical potential of water outside of MLV becomes lower than that of inside of MLV, that is, the osmotic stress acts on the MLV. In an equilibrium state, the osmotic stress is counterbalanced by the elastic pressure which lowers the chemical potential of water inside of MLV, and consequently, all the lipid bilayer membranes in the MLV are equally compressed. Membrane fluidity decrease under the osmotic stress was detected by electron spin resonance method [8]. Thermodynamical analysis showed that the lateral pressure f in the membranes increases with an increase in the osmotic stress C_{osm} according to below equation [11]:

$$f = (1/n_l)(\partial V_w/\partial S_l)C_{osm}$$

where n_l is the number of bilayers in the vesicle and V_w is the volume of water inside the vesicle

and S_1 is the surface area of the bilayer. Therefore the lateral packing of the lipid molecules becomes denser at higher concentration of PEG. It is well recognized that the phase transition temperature increases as the lateral packing density or surface pressure increases [22–24]. Hence the osmotic stress enhances the phase transition temperature owing to the increase in the lateral packing.

It is well known that hydrostatic pressure raises the phase transition temperature of MLV in accordance with the Clausius–Clapeyron equation [25,27]. Hence it is valuable to compare the effect of the osmotic stress on the phase transition with that of the hydrostatic pressure.

The increase of T_m depended on the hydrocarbon chain length (Fig. 3). The shorter the alkyl chain length is, the larger the increment is. This dependence was larger than that in the case of hydrostatic pressure, where the longer the alkyl chain is, the larger the increment is. (The values of dT_m/dP were 23.0°C/kbar for DMPC-MLV and DPPC-MLV and 28.0°C/kbar for DSPC-MLV under hydrostatic pressure [25].) The abrupt increase of ΔH at 48% (w/v) PEG 6K may be due to the overlap of the main transition and the pre-transition peaks, because pre-transition peak disappeared above 48% (w/v) and the increment of ΔH at 48% (w/v) was almost equal to the enthalpy change of pre-transition. Consequently, the enthalpy change of main transition did not significantly change under the osmotic stress. A similar situation exists in the presence of hydrostatic pressure (up to 136 atm) [25]; the increase of ΔH by osmotic stress or hydrostatic pressure may be very small compared with ΔH in the pure PC-MLV. Osmotic stress increased the half width of the main transition temperature peak. This result might mean that the transition under osmotic stress conditions was less cooperative in nature than in absence of osmotic stress. It contrasted with the effect of hydrostatic pressure [25].

The main difference between the response of phospholipid-MLV to osmotic stress and hydrostatic pressure is best explained as follows. In the former case, water moves from inside of the MLV, that is, both the region between bilayers and the inside of bilayers, to the outside (bulk phase). Small-angle X-ray scattering data indicated that the lamellar repeat distance and interbilayer distance of phopholipid-MLV decreased with an increase in osmotic stress [26]. This phenomenon is similar to the response of gels to osmotic stress. For example, the response of Sephadex gel to osmotic stress was investigated quantitatively [13]. On the other hand, in the response of phospholipid-MLV to hydrostatic pressure, water does not move from inside of the MLV. Neutron diffraction study indicated that the lamellar repeat distance of DPPC-MLV in the liquid-crystalline state slightly increased with an increase in hydrostatic pressure [27]. There might exist, therefore, some differences between the elastic response of lipid bilayer membranes in the MLV to the osmotic stress and that resulting from hydrostatic pressure, so that the effect of osmotic stress on phase transition of MLVs might differ from that of hydrostatic pressure.

The dependence of phase transition temperature on water contents has been studied by DSC [28,29]. At low content of water ($\lesssim 30\%$ w/w), T_m increased with a decrease in water content. This phenomenon can be explained as follows. The lamellar repeating period of neutral phospholipid-MLV increased as the water content increased up to constant value C_w ($30 \sim 40\%$, depending on temperature) above which it did not change [30,31]. These data show that MLV swells up to the C_w and it reaches an equilibrium state such as the phenomena of swelling of the gels [32,33]. Therefore the chemical potential of water in the MLV is smaller than that of pure water below C_w and it decreases with a decrease in water content [26]. This situation is the same as that of MLV under osmotic stress. At low concentration of water, membranes are compressed to decrease the chemical potential of water. Electron density profiles of bilayers of DPPC-MLV and egg PC-MLV showed that the thickness of the bilayer increased and thereby the lateral packing increased with a decrease in water content [34]. Hence the increase of the phase transition temperature at low contents of water might be due to the increase in lateral packing density of membranes.

Ethylene glycol monomer had a biphasic effect on the transition temperature of DPPC-MLV, reducing T_m a little (almost no effect) and T_p largely at low concentrations but increasing T_m and extinguishing the pre-transition at high concentrations. The reduction of transition temperature at low EG concentrations can be explained by the same theory applied for freezing point depression calculations [35], since more EG molecules partition in the L_α phase than in the gel phase. Deuterium-NMR studies showed that EG changed choline head group conformation and induced alkyl chain disordering in the L_α phase of phosphatidyl-choline membrane, which indicated that EG molecules penetrate into both the head group region and the hydrocarbon region [36,37].

A sudden and large decrease (15 Å) of the repeating period at 36% (w/v) EG indicates the induction of a new phase of MLV and the large decrease of the bilayer thickness. The electron density profiles of DPPC-MLV at high concentration of EG shows that the bilayer thickness is 30 Å (unpublished results, [38]). A single sharp reflection in the wide-angle X-ray pattern means that the lipid hydrocarbon chains are perpendicular to the plane of the bilayer. These structures are characteristic of the interdigitated gel phase ($L_{\beta I}$) observed under the high pressure [27] and at high concentration of ethanol [19]. The induction of $L_{\beta I}$ phase of DPPC-MLV at low water content by 39% EG has previously been reported [38]. Our new results are the determination of temperature–EG concentration phase diagram at excess water and the chain length dependence of this diagram.

Phase diagrams of temperature–EG concentration for PC-MLV were similar to those of temperature–ethanol concentration which was determined by the automated scanning density meter [39]. There were three regions in these phase diagrams. In Region A (low concentrations of EG), T_p decreased more largely than T_m with an increase in EG concentration. In Region B (medium concentrations of EG), $L_{\beta I}$ phase was induced between $L_{\beta'}$ and $P_{\beta'}$ phases. In Region C (high concentrations of EG), T_m increased and the phase transition temperature from $L_{\beta'}$ to $L_{\beta I}$ phase decreased with an increase in EG concentration. The phenomena observed in Region C can be explained as follows. More EG molecules are partitioned into the membrane in the $L_{\beta I}$ phase than in the $L_{\beta'}$ and L_α phases, since the hydrocarbon chains in the $L_{\beta I}$ phase face the aqueous phase and, as a consequence, there are more binding sites of EG. (See for a similar discussion in the case of ethanol, Ref. [19].) The order of magnitude of the partition coefficients of EG into the membrane is $L_{\beta I} > L_\alpha > L_{\beta'}$. Hence, the phenomena in Region C can be explained by this order of the partition coefficients similarly to the theory for freezing point depression. The EG concentration where the phase transition from $L_{\beta'}$ to $L_{\beta I}$ phase occurs along isotherms depends on the temperature and it increases as the temperature decreases. This tendency resembles that of the temperature–pressure phase diagram [27].

The chain length dependence of the minimum concentration of EG where interdigitation occurs was the same as that of ethanol-induced interdigitation and can be explained reasonably by the chain length dependence of the stability of $L_{\beta I}$ phase just as in the case of ethanol-induced interdigitation [19].

The formation of $L_{\beta I}$ phase also indicates that EG can easily penetrate into the head group region of the lipid (exclusion layer) in the gel phase MLV, because of a small size of the EG molecule, in contrast with PEG 6K. As discussed in a previous paper [8], for its larger molecular weight, PEG would be excluded more effectively from the exclusion layer of the membrane and produce larger osmotic stress. The monomeric EG will, however, induce little osmotic stress onto the membrane.

Acknowledgments

We thank Professor T. Yoshida of Shizuoka university for helpful discussions. Part of this work was presented at the 27th Annual Meeting of the Biophysical Society of Japan, September, 1989, Tokyo. This work was partly supported by Grant-in-Aid from the Ministry of Education, Science and Culture of Japan.

References

1 K.N. Kao, F. Constable, M.R. Michayluck and O.L. Gamborg, Planta 120 (1974) 215–227.
2 Q.F. Ahkong, D. Fisher, W. Tampion and J.A. Lucy, Nature 253 (1975) 194–195.
3 R.L. Davidson and P.S. Gerald, Somatic Cell Genet. 2 (1976) 165–176.
4 J.A. Lucy, in: Structure of biological membranes, eds. S. Abrahamson and I. Pascher (Plenum Press, New York, NY, 1977).
5 C.P.S. Tilcock and D. Fisher, Biochim. Biophys. Acta 688 (1982) 645–652.
6 L.T. Boni, J.L. Alderfer and S.W. Hui, J. Membr. Biol. 62 (1981) 65–70.
7 R. Saez, A. Alonso, A. Villena and F.M. Goni, FEBS Lett. 137 (1982) 323–326.
8 M. Yamazaki, S. Ohnishi and T. Ito, Biochemistry 28 (1989) 3710–3715.
9 M. Yamazaki and T. Ito, Biochemistry 29 (1990) 1309–1314.
10 C.P.S. Tilcock and D. Fisher, Biochim. Biophys. Acta 577 (1979) 53–61.
11 T. Ito, M. Yamazaki and S. Ohnishi, Biochemistry 28 (1989) 5626–5630.
12 A. Suzuki, M. Yamazaki and T. Ito, Biochemistry 28 (1989) 6513–6518.
13 T. Ito, M. Yamazaki and S. Ohnishi, Biophys. J. 56 (1989) 707–711.
14 M. Yamazaki, M. Ohshika and T. Ito, Biochim. Biophys. Acta 1063 (1991) 175–177.
15 G.R. Bartlett, J. Biol. Chem. 234 (1959) 466–468.
16 D. Chapman, in: Form and function of phospholipids, eds. G.B. Ansell, J.N. Hawthorne and R.H.C. Dawson (Elsevier, Amsterdam, 1973) pp. 117–142.
17 S.C. Chen, J.M. Sturtevant and B.J. Gaffney, Proc. Natl. Acad. Sci. USA 77 (1980) 5060–5063.
18 A. Tardieu, V. Luzati and F.C. Reman, J. Mol. Biol. 75 (1973) 711–733.
19 S.A. Simons and T.J. McIntosh, Biochim. Biophys. Acta 773 (1984) 169–172.
20 S. Aruga, R. Kataoka and S. Mitaku, Biophys. Chem. 21 (1985) 265–275.
21 K. Arnold, O. Zschoernig, D. Barthel and W. Herold, Biochim. Biophys. Acta 1022 (1990) 303–310.
22 F. Jähnig, Biophys. J. 36 (1981) 329–345.
23 J.C. Owicki, M.W. Springgate and H.M. McConnell, Proc. Natl. Acad. Sci. USA 75 (1978) 1616–1619.
24 E. Sackmann in: Biophysics, ed. W. Voppe (Springer Verlag, Berlin, 1983) pp. 425–457.
25 D.B. Mountcastle, R.L. Biltonen and M.J. Halsey, Proc. Natl. Acad. Sci. USA 75 (1978) 4906–4910.
26 D.M. LeNeveu, R.P. Rand and V.A. Parsegian, Biophys. J. 18 (1977) 209–230.
27 L.F. Braganza and D.L. Worcester, Biochemistry 25 (1986) 2591–2596.
28 R.M. Williams and D. Chapmann, Prog. Chem. Fats Other Lipids, 33 (1970) 3–74.
29 M.J. Janiak, D.M. Small and G.G. Shipley, J. Biol. Chem. 254 (1979) 6068–6078.
30 D. Chapmann, R.M. Williams and B.D. Ladbrooke, Chem. Phys. Lipids 1 (1967) 445–475.
31 R.P. Rand, Annu. Rev. Biophys. Bioeng. 10 (1981) 277–314.
32 P.J. Flory, Principles of polymer chemistry (Cornell University Press, Ithaca, NY, 1953).
33 T. Tanaka, D. Fillmore, S.T. Sun, I. Nishio, G. Swislow and A. Shah, Phys. Rev. Lett. 40 (1980) 820–823.
34 J. Torbet and M.H.F. Wilkins, J. Theor. Biol. 62 (1976) 447–458.
35 M.W. Hill, Biochim. Biophys. Acta 356 (1974) 117–124.
36 K. Nicolay, E.B. Smaal and B. Kruijff, FEBS Lett. 209 (1986) 33–36.
37 B. Bechinger, P.M. Macdonald and J. Seelig, Biochim. Biophys. Acta 943 (1988) 381–385.
38 R.V. McDaniel, T.J. McIntosh and S.A. Simon, Biochim. Biophys. Acta 731 (1983) 97–108.
39 K. Ohki, K. Tamaura and I. Hatta, Biochim. Biophys. Acta 1028 (1990) 215–222.
40 W. Li, T.S. Aurora, T.H. Haines and H.Z. Cummins, Biochemistry 25 (1986) 8220–8229.
41 S.-T. Sun, A. Milon, T. Tanaka, G. Ourisson and Y. Nakatani, Biochim. Biophys. Acta 860 (1986) 525–531.